

This article was downloaded by: [Tomsk State University of Control Systems and Radio]

On: 23 February 2013, At: 04:48

Publisher: Taylor & Francis

Informa Ltd Registered in England and Wales Registered Number: 1072954

Registered office: Mortimer House, 37-41 Mortimer Street, London W1T 3JH, UK



## Molecular Crystals and Liquid Crystals

Publication details, including instructions for authors and subscription information:

<http://www.tandfonline.com/loi/gmcl16>

### Vibronic Absorption with Totally Symmetrical Phonons in Naphthalene Crystal

T. A. Krivenko<sup>a</sup>, E. F. Sheka<sup>a</sup> & E. I. Rashba<sup>b</sup>

<sup>a</sup> Institute of Solid State Physics, Academy of Sciences of the USSR, Chemogolovka, 142432, USSR

<sup>b</sup> L. D. Landau Institute of Theoretical Physics, Academy of Sciences of the USSR, Chemogolovka, 142432, USSR

Version of record first published: 28 Mar 2007.

To cite this article: T. A. Krivenko, E. F. Sheka & E. I. Rashba (1978): Vibronic Absorption with Totally Symmetrical Phonons in Naphthalene Crystal, *Molecular Crystals and Liquid Crystals*, 47:3-4, 119-143

To link to this article: <http://dx.doi.org/10.1080/00268947808083738>

PLEASE SCROLL DOWN FOR ARTICLE

Full terms and conditions of use: <http://www.tandfonline.com/page/terms-and-conditions>

This article may be used for research, teaching, and private study purposes. Any substantial or systematic reproduction, redistribution, reselling, loan, sub-licensing, systematic supply, or distribution in any form to anyone is expressly forbidden.

The publisher does not give any warranty express or implied or make any representation that the contents will be complete or accurate or up to date. The accuracy of any instructions, formulae, and drug doses should be

independently verified with primary sources. The publisher shall not be liable for any loss, actions, claims, proceedings, demand, or costs or damages whatsoever or howsoever caused arising directly or indirectly in connection with or arising out of the use of this material.

# Vibronic Absorption with Totally Symmetrical Phonons in Naphthalene Crystal

T. A. KRIVENKO and E. F. SHEKA

*Institute of Solid State Physics, Academy of Sciences of the USSR, Chernogolovka, 142432, USSR*

and

E. I. RASHBA

*L. D. Landau Institute of Theoretical Physics, Academy of Sciences of the USSR, Chernogolovka, 142432, USSR*

(Received January 16, 1978)

We present the first quantitative analysis of the vibronic spectrum with totally symmetrical phonon based on the dynamical theory of vibronic spectra. Calculation of the fundamental absorption spectrum, carried out for the naphthalene crystal, allowed the description of absorption in the region of the first vibronic transition  $K_1$  and the determination of the parameters of the exciton-phonon interaction hamiltonian. As applied to the crystal with isotopic impurity, the calculation revealed the existence of definite series in the impurity-vibronic complex spectrum: two terms of the series are found experimentally. Also the application of the theory to compound vibronic spectra involving two intramolecular phonons turned out very successful.

## 1 INTRODUCTION

Most of bands in exciton absorption spectra of molecular crystals correspond to vibronic transitions when an exciton and one or more internal phonons are simultaneously created. The intensity distribution in the vibronic spectrum is determined entirely by interactions in the final state, that is, by the interaction of the exciton with phonons created simultaneously with it. The exciton-phonon interaction is not generally weak, and the dimensionless coupling constant is about unity for most intensive vibronic transitions defining the principal features of the spectrum. In many cases this interaction turns out to be sufficient to produce bound exciton-phonon states. Under such conditions, usual perturbation theory in the coupling constant is certainly inapplicable.

So, the analytic theory can only be developed for the case when another small parameter is found.

The assumption that the parameter  $\varepsilon_{\text{ex}}/\nu \ll 1$  is small ( $\varepsilon_{\text{ex}}$  is the exciton band width and  $\nu$  is the phonon frequency) forms the basis of the dynamical theory of vibronic spectra developed by one of the authors<sup>1</sup> and then considered in a number of papers (see, for example, Refs. 2, 3, and 4). Using the smallness of this parameter, one can derive the exciton-phonon hamiltonian conserving the number of phonons. This hamiltonian allows practically complete solution of the problem, namely, finding the bound states of exciton and phonon (one-particle states), the intensities of corresponding transitions and the intensity distribution in the dissociated (two-particle) state spectrum. Inequality  $\varepsilon_{\text{ex}}/\nu \ll 1$  is fulfilled for the predominant majority of molecular crystals. Owing to this the dynamical theory can be widely used for the quantitative interpretation of experimental spectra. Apart from the dynamic theory, only definite interpolation schemes are accessible. One described in Ref. 5 appears to be the most effective.

The qualitative analysis of experimental data carried out on the basis of the dynamical theory, at first for one of vibronic transitions in naphthalene,<sup>6</sup> and then for the two first intensive transitions in benzene, naphthalene and anthracene<sup>7</sup> gave quite favourable results.

Quantitative comparison between theory and experimental data has been made by now for neat and impure naphthalene crystals<sup>8,9</sup> for the transition which corresponds to the non-totally symmetrical (NTS) phonon  $b_{3g}$  with frequency  $509 \text{ cm}^{-1}$ . Even though the situation in the two-particle absorption region is rather complicated by the external phonon contribution, the agreement between theory and experiment is quite satisfactory.

However, totally symmetrical (TS) internal phonons are of the greatest interest, from the point of view of dynamical theory, because the hamiltonian of the TS-phonon interaction with exciton has a very peculiar non-local form. In the present paper, the naphthalene vibronic absorption spectrum involving the TS-phonon is calculated. The results describe rather well the experimental spectra<sup>10,11</sup> of perproto  $d_0$  and perdeutero  $d_8$  naphthalene in the region of  $K_1$ -transition.<sup>†</sup> In conclusion, impurity crystal spectra and two-phonon spectra are also discussed.

<sup>†</sup> Hereafter we denote the vibronic spectrum regions including  $n$  TS phonons as  $K_n$ . The strongly polarized one-particle absorption bands we denote as  $A_n$  and  $B_n$  to indicate their polarization. So, the pure electron exciton doublet is denoted as  $K_0$ , and the corresponding bands as  $A_0$  and  $B_0$ . The vibronic one-particle absorption doublet in the  $K_1$ -region is denoted as  $A_1$  and  $B_1$ , and in the  $K_2$ -region—as  $A_2$  and  $B_2$ , etc. In this paper our notations differ from those used in earlier works where the exciton doublet was denoted as  $A_1$  and  $B_1$ , the first vibronic one as  $A_2$  and  $B_2$ , etc. Vibronic absorption one-particle bands with one NTS phonon we shall denote through  $M$  as before.

## 2 GENERAL APPROACH

The dynamical theory<sup>1</sup> hamiltonian in the site representation has the form when counting off the electronic term

$$H = H_{\text{ex}} + H_{\text{ph}} + H_{\text{int}}^{(1)} + H_{\text{int}}^{(2)} \quad (1)$$

where

$$H_{\text{ex}} = \sum_{n\alpha \neq m\beta} M_{n\alpha m\beta} a_{n\alpha}^+ a_{m\beta}, \quad H_{\text{ph}} = \nu_0 \sum_{n\alpha} b_{n\alpha}^+ b_{n\alpha}, \quad (2)$$

$$H_{\text{int}}^{(1)} = \Delta \sum_{n\alpha} a_{n\alpha}^+ a_{n\alpha} b_{n\alpha}^+ b_{n\alpha}, \quad (3)$$

$$H_{\text{int}}^{(2)} = \gamma^2 \sum_{n\alpha \neq m\beta} M_{n\alpha m\beta} a_{n\alpha}^+ a_{m\beta} \{b_{n\alpha}^+ b_{m\beta} + b_{m\beta}^+ b_{n\alpha} - b_{n\alpha}^+ b_{n\alpha} - b_{m\beta}^+ b_{m\beta}\} \quad (4)$$

The first two terms are the free exciton and the free phonon hamiltonians:  $\nu_0$  is the vibrational frequency of the molecule in its electronic ground state. The term  $H_{\text{int}}^{(1)}$  describes the exciton-phonon interaction caused by the change in vibrational frequency (by  $\Delta < 0$ ) under molecule electronic excitation. This interaction is quadratic and exists for phonons with any symmetry. The term  $H_{\text{int}}^{(2)}$  owes its origin to the linear exciton-phonon interaction, which leads to the oscillator equilibrium position displacement under molecule electronic excitation:  $\gamma$  is the dimensionless constant corresponding to this interaction. When  $|M_{n\alpha m\beta}| \ll \nu_0$ , the linear interaction hamiltonian (which does not conserve the number of phonons) may be reduced to hamiltonian (4), conserving the number of phonons.

In the Condon approximation, the renormalized matrix elements of the resonance interaction  $M_{n\alpha m\beta}$  are connected with the pure electronic matrix elements  $M_{n\alpha m\beta}^0$  by the Debye-Waller factor  $e^{-\gamma^2}$ :

$$M_{n\alpha m\beta} = M_{n\alpha m\beta}^0 e^{-\gamma^2} \quad (5)$$

The total intensity of the vibronic transition  $I_1$  corresponding to one exciton and one phonon creation is simply related to the intensity of the pure electronic transition  $I_0$ :

$$I_1 = \gamma^2 I_0 \quad (6)$$

The values  $\gamma$  and  $\Delta$  are intramolecular constants. If they are known from the experiments on vapour or impurity spectra, the exciton-phonon interaction hamiltonian does not contain any unknown parameters and is fully determined by resonance integrals  $M_{n\alpha m\beta}$  associated with the exciton spectrum dispersion law.

Hamiltonian (1)–(4) has always continuous spectrum, corresponding to two-particle states of the exciton + phonon pair. This spectrum coincides in width with the exciton band width. If the exciton–phonon interaction is sufficiently strong, then along with two-particle states the one-particle states, that is, bound states of the exciton + phonon pair, may arise. One-particle states are to be correlated with narrow bands of a vibronic absorption spectrum.

Intensity distribution in the two-particle spectrum is determined by the exciton–phonon interaction. For NTS phonons the constant  $\gamma = 0$  and the interaction is reduced to  $H_{\text{int}}^{(1)}$ . In this case the two-particle absorption spectrum is directly expressed through  $\rho(\omega)$ —the density-of-state in the exciton band. To solve the problem for TS phonons, one should know the exciton spectrum dispersion law  $\epsilon_\mu(\mathbf{k})$ ; index  $\mu$  numbers the exciton bands.

The density-of-state  $\rho(\omega)$  in the exciton band of naphthalene crystal has been found so far with satisfactory accuracy by analyzing the whole set of experimental data (Figure 1). It is also known that the matrix element  $M_{12} \approx 20 \text{ cm}^{-1}$  dominates among the other resonance integrals. It corresponds to the interaction of adjacent translationally non-equivalent molecules in the crystal **ab**-plane. To keep only this integral is equivalent to pass to the layer lattice. However  $\rho(\omega)$  constructed in such a model deviates greatly from the experimental one (see Figure 1). This shows that other integrals are also significant. Unfortunately our knowledge of their values is insufficient at present. Three sets of the integrals proposed in Ref. 13 are completely different from each other though all these sets describe the  $\rho(\omega)$  rather well. So only

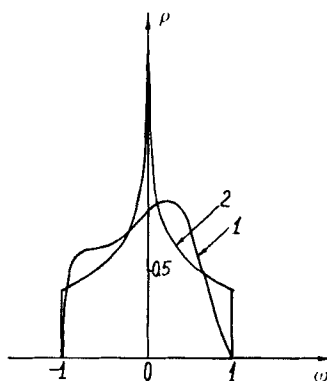


FIGURE 1 Exciton density-of-states of the lowest electronic transition  ${}^1B_{2u}$  of the naphthalene crystal. The half-width of band  $90 \text{ cm}^{-1}$  is taken as unity. 1. Experimental density-of-state as the result of data processing for isotope-impurity crystals.<sup>8</sup> The centre of gravity position  $\epsilon_g = -84 \text{ cm}^{-1}$  is measured from the bottom of the band. 2. Result of calculation in the approximation of the nearest neighbour interaction,  $M_{12} = 22.5 \text{ cm}^{-1}$  (features in the band centre and on the edges are due to the two-dimensional model).

$\rho(\omega)$  and  $M_{12}$  will be used in our calculations. Doing so one can believe to obtain a reasonable description of the general picture rather than the reproduction of details.

There is a specific feature of the naphthalene spectrum which gives rise to marked complications and requires a special discussion. The first electronic transition of the naphthalene molecule  $A_{1g} \rightarrow {}^1B_{2u}$  is very weak; its oscillator strength in vapour is  $f_{B_{2u}}^0 = 10^{-4}$ .<sup>14</sup> Its value in the crystal rises to  $f_{B_{2u}} \approx 2 \cdot 10^{-2}$  (Ref. 10) due to mixing with the second transition  ${}^1B_{3u}$  (Ref. 15) having oscillator strength  $f_{B_{3u}} \approx 0.1$ . The second transition is close to the first one: in vapour the distance between them is equal to  $E_{12} \approx 3900 \text{ cm}^{-1}$ ,<sup>17</sup> and in the crystal it is reduced to  $E_{12} \approx 2180 \text{ cm}^{-1}$ .<sup>18</sup> The frequency of the TS vibration  $\nu_0$  ( $761 \text{ cm}^{-1}$ ) corresponding to the vibronic absorption  $K_1$  is comparable with  $E_{12}$ . But for  $\nu_0 \sim E_{12}$  the configuration admixing of the second electronic transition is different for electronic and vibronic components of the first electronic transition. So, the theory,<sup>1</sup> constructed for the isolated transition, is not directly applicable to it.

There is, however, a favourable circumstance which simplifies the problem and makes its treatment fairly accessible. It is based on the fact that the ratio  $f_{B_{2u}}/f_{B_{3u}} \approx 0.2 \ll 1$ . This makes it possible to consider the interlevel mixing as comparably small (admixture of  $\psi_{B_{3u}}$  to  $\psi_{B_{2u}}$  is about  $\beta \approx 0.4$ ). The great change in the oscillator strength  $f_{B_{2u}}/f_{B_{2u}}^0 > 100$  is due simply to enormous difference in the oscillator strength of both transitions in the free molecule ( $f_{B_{2u}}^0/f_{B_{3u}}^0 \approx 0.001$ ). If the contribution of dipole-dipole interactions to the exciton band width is not too large† and  $\beta$  is small, then quasi-particle dynamics will be described by hamiltonian (1)–(4) as before. It can be shown that in this case it will describe properly the intensity distribution in the vibronic spectrum (including one- and two-particle spectrum) as well. In what follows, we shall confine ourselves to this approximation. But the integrated intensity of vibronic absorption is not determined by formula (6) in this case; it depends, due to configuration mixing, on the exciton-phonon interaction constants for both electronic transitions. The fact that for  $E_{12} \sim \nu_0$  different vibronic levels mix independently with the second electronic transition has been noted in Ref. 11.

### 3 VIBRONIC ABSORPTION SPECTRUM CALCULATION

In the dynamical theory the vibronic absorption spectrum corresponding to the excitation of one phonon is described by the two-particle exciton-phonon

† The quantitative theory of naphthalene exciton band is not available. But, taking into account the oscillator strength value, the band is likely formed chiefly due to higher multipole interactions, and the contribution of dipole-dipole interactions is of the order of  $10^0\%$ .

Green function. In the electro-dipole approximation, the conductivity tensor describing directly the absorption has the form:

$$\hat{\sigma}(\omega) = -\frac{e^2}{vm\omega} \text{Im} \sum_{\alpha\beta} F_{\alpha\beta}(\omega) \widehat{\mathbf{P}_\alpha \cdot \mathbf{P}_\beta} \quad (7)$$

Here  $v$  is the unit cell volume,  $\mathbf{P}_\alpha$  is the dipole moment of the intramolecular vibronic transition in molecules of sublattice  $\alpha$  (corrected for configuration mixing) and  $F_{\alpha\beta}(\omega)$  is the two-particle exciton-phonon Green function at the zero total momentum.

The function  $F_{\alpha\beta}(\omega)$  is generally expressed through the exciton-phonon vertex  $\Gamma_{\alpha\beta\gamma\delta}(\mathbf{k}_1, \mathbf{k}_2)$  (Figure 2). The method of solving the equation for the vertex, proposed in Ref. 1, is based on the fact that  $\Gamma$ , and hence  $F$ , can be rather simply expressed through the vertex  $\bar{\Gamma}$  for the auxiliary problem in which the exciton-phonon interaction reduces to the second term in Eq. (4), i.e., to the exchange-resonance interaction of the type  $a_{n\alpha}^+ a_{m\beta} b_{m\beta}^+ b_{n\alpha}$ . The infinite equation system for the vertex  $\bar{\Gamma}_{\alpha\beta\gamma\delta}(\mathbf{n}, \mathbf{m})$  is truncated in the site representation, if the interaction with only a finite number of neighbours is considered.

We have solved this system for the naphthalene type lattice including only the interaction with the nearest translationally nonequivalent neighbours  $M_{12} \equiv M$  and have calculated the matrix  $F_{\alpha\beta}$ . The conductivity tensor components  $\sigma_\lambda$ , determining the spectrum in the two principal directions in the  $\mathbf{ab}$  plane are determined, with allowance made for sublattice equivalence, by expressions

$$F_\lambda(\omega) = F_{11}(\omega) + (-1)^\lambda F_{12}(\omega) = \frac{f(0, \omega) + 4f^2\left(\frac{\mathbf{a} + \mathbf{b}}{2}, \omega\right) y_\lambda(\omega)}{\Phi_\lambda(\omega)} \quad (8)$$

Here  $\lambda = 1, 2$  correspond to the electric vector polarization along  $a$  and  $b$  axes,

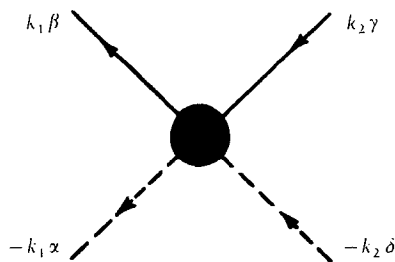


FIGURE 2 Exciton-phonon vertex  $\Gamma_{\alpha\beta\gamma\delta}(k_1, k_2)$ .



**a** and **b** are the primitive translations in these directions. The function  $f$  is defined by

$$f(\mathbf{l}, \omega) = v \sum_{\mu} B_{\alpha}^{\mu} B_{\beta}^{\mu} \int \frac{d^3 \mathbf{k}}{(2\pi)^3} \frac{e^{i\mathbf{k}\mathbf{l}}}{\omega - \varepsilon_{\mu}(\mathbf{k}) + i0} \quad (9)$$

for any lattice vector  $\mathbf{l}$  joining the  $\alpha$  type molecule with that of the  $\beta$  type; summation is over both exciton bands,  $B_{\alpha}^{\mu}$  are known phase factors. Here and thereafter, two different energy scales are used to simplify the formulae. In the quantities connected with the vibronic transition, such as  $F_{\alpha}(\omega)$ , frequencies are always counted off the vibronic term  $\varepsilon_0 + \nu_0$ . On the contrary, all the values connected with the pure electron transition— $\varepsilon_{\mu}(\mathbf{k})$  and  $\rho(\omega)$ —are counted off the electron term  $\varepsilon_0$ . With such a reading, two-particle spectrum edges coincide with the edges of the region  $\rho(\omega) \neq 0$ .

Functions  $y_{\lambda}$  are equal to

$$y_{\lambda} = \frac{\gamma^2 M}{(-1)^{\lambda} - \gamma^2 M \varphi}, \quad (10)$$

and functions  $\Phi_{\lambda}$  are equal to

$$\begin{aligned} \Phi_{\lambda}(\omega) = & \left\{ 1 - (-1)^{\lambda} 4f\left(\frac{\mathbf{a} + \mathbf{b}}{2}, \omega\right) y_{\lambda} \right\}^2 \\ & - \left\{ f(0, \omega) + 4f^2\left(\frac{\mathbf{a} + \mathbf{b}}{2}, \omega\right) y_{\lambda} \right\} \\ & \times \{ \Delta + (-1)^{\lambda} 4\gamma^2 M(1 + 4\varphi y_{\lambda}) \}, \end{aligned} \quad (11)$$

where

$$\varphi(\omega) = f(0, \omega) + f(\mathbf{a}, \omega) + f(\mathbf{b}, \omega) + f(\mathbf{a} + \mathbf{b}, \omega) \quad (12)$$

In the model of the nearest neighbour interaction the various  $f(\mathbf{l}, \omega)$  are not independent. In particular,

$$f\left(\frac{\mathbf{a} + \mathbf{b}}{2}, \omega\right) = \frac{\omega f(0, \omega) - 1}{4M}, \quad \varphi(\omega) = \frac{\omega(\omega f(0, \omega) - 1)}{4M^2}, \quad (13)$$

These formulae together with Eqs. (8)–(12) enable the absorption spectrum to be directly expressed through the  $f(0, \omega)$ . This last integral does not depend on the details of the dispersion law  $\varepsilon_{\mu}(\mathbf{k})$ , but is fully determined by the density-of-state  $\rho(\omega)$  in the exciton energy spectrum  $\text{Im } f(0, \omega) = -\pi\rho(\omega)$ ;  $\rho(\omega)$  is normalized to unity. Thus, in the scheme adopted, the absorption spectrum is determined by the values  $\Delta$ ,  $\gamma$ ,  $M$  and function  $\rho(\omega)$ . The direct application of formula (9) to the model of the nearest neighbour interaction would lead to a singular  $\rho(\omega)$  (Figure 1, curve 2). So, it would be more reasonable to take advantage of the experimental curve  $\rho(\omega)$  for the three-dimensional crystal.

Such a combination of the nearest neighbour model with the use of the experimental  $\rho(\omega)$  has been used earlier<sup>19</sup> rather successfully when calculating defect impurity states. So, one can hope that such an approach will lead in our case to satisfactory results, as well. The comparison of integrals  $f(l, \omega)$  found in this way with that calculated in Ref. 13 by a more sophisticated dispersion law, shows that, as a whole, they are similar.

For the calculation results to be applied in the future to the analysis of naphthalene spectrum, curve 1 of Figure 1 is taken as  $\rho(\omega)$ . The value of  $M$  is taken as  $180/8 = 22.5 \text{ cm}^{-1}$  so as to give a correct value of the exciton spectrum width: it is close to the values obtained by other methods. The frequency change  $\Delta$  is known only for vapour ( $\Delta = -59 \text{ cm}^{-1}$ ).<sup>14</sup> For the crystal this value may change somewhat (as it is, e.g., the case with the NTS phonon  $\nu_0 = 509 \text{ cm}^{-1}$ ).<sup>8</sup> Therefore, we shall not assume below that  $\Delta$  remains unchanged. The value  $\gamma$  is not known at all due to a large contribution of the configuration mixing effect to the absorption intensity. We shall try in the future to determine it by fitting the calculated and the experimental data.

#### 4 THE $\kappa_1$ REGION: CALCULATION AND COMPARISON WITH EXPERIMENT

In order to gain general insight into the structure of the spectrum we shall start with describing the calculation results of the spectrum as a function of parameters  $\Delta$  and  $\gamma$ .

The position of  $\delta$ -shaped one-particle absorption bands is determined by the isolated poles of the functions  $F_\lambda(\omega)$  (cf. (8)), i.e., by the roots of the equation

$$\Phi_\lambda(\omega_\lambda) = 0 \quad (14)$$

Frequencies  $\omega_\lambda$  determine the positions of one-particle bands and lie off the energy region corresponding to two-particle excitations.

Figure 3 shows the dependence of Eq. (14) solutions  $\omega_\lambda$  on  $\Delta$ . We consider only the case of negative  $\Delta$  since this very case corresponds to the experimental situation. For negative  $\Delta$ , one-particle bands lie in the frequency region below the lower edge of two-particle absorption. The curves in Figure 3 correspond to definite values  $\gamma^2$ . The case of  $\gamma^2 = 0$  (curve 0) corresponds to the interaction of exciton with NTS phonon which was investigated earlier.<sup>8</sup> In this case Eq. (14) reduces to the well known equation

$$\Delta \int \frac{\rho(\omega') d\omega'}{\omega - \omega'} = 1 \quad (15)$$

As has been shown earlier in Ref. 8, the solution of this equation with the

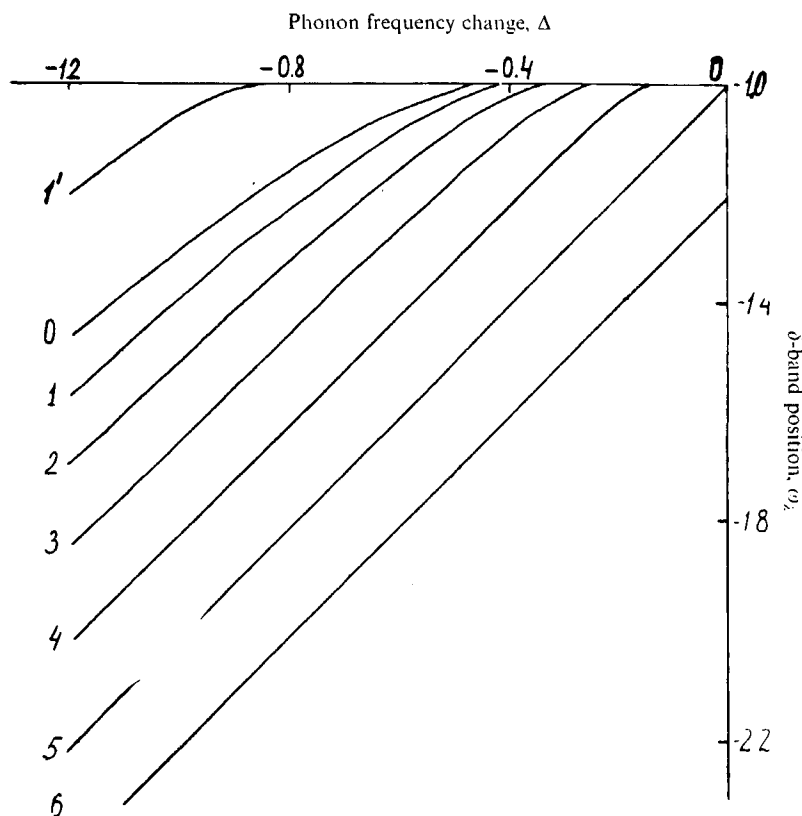


FIGURE 3 Position of  $\delta$ -shaped bands of one-particle vibronic absorption  $\omega_\delta$  depending on the phonon frequency change  $\Delta$ . The frequency change and band position are given in units of the exciton band half-width. The curves correspond to the following  $\gamma^2$  values: 0-0; 1' and 1-0.2; 2-0.4; 3-0.6; 4-0.8; 5-1.0; 6-1.2.

experimental density-of-state  $\rho(\omega)$  describes quantitatively the position of the one-particle states exciton + NTS phonon and the impurity levels in deuterionaphthalenes isotope-impurity crystals.

At  $\gamma^2 \neq 0$  Eq. (14) are not the same for two spectrum components ( $\lambda = 1, 2$ ), polarized along **a** and **b** crystal axes. The curves located under the curve with  $\gamma^2 = 0$  correspond to the first case, and those located above it correspond to the second case. From Figure 3 it is seen that one-particle excitations arise only for  $|\Delta|$  larger than some critical value  $|\Delta_{cr}^\lambda|$ . The critical value  $|\Delta_{cr}^1|$  for the *a*-component is less than  $|\Delta_{cr}^2|$  for the *b*-polarized bands. Therefore, for some region of values  $\Delta$ , the one-particle band arises only in the *a*-component, i.e., the vibronic multiplet of one-particle absorption is incomplete as opposed

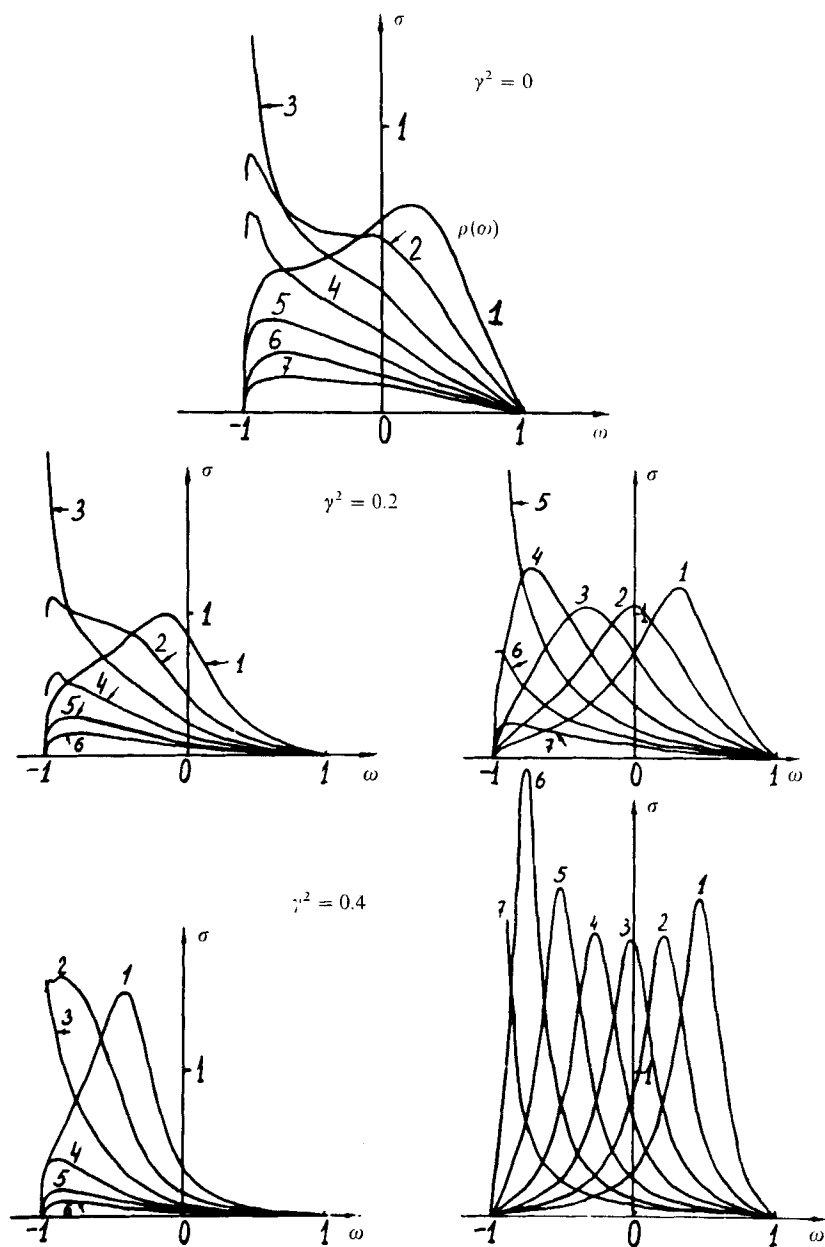
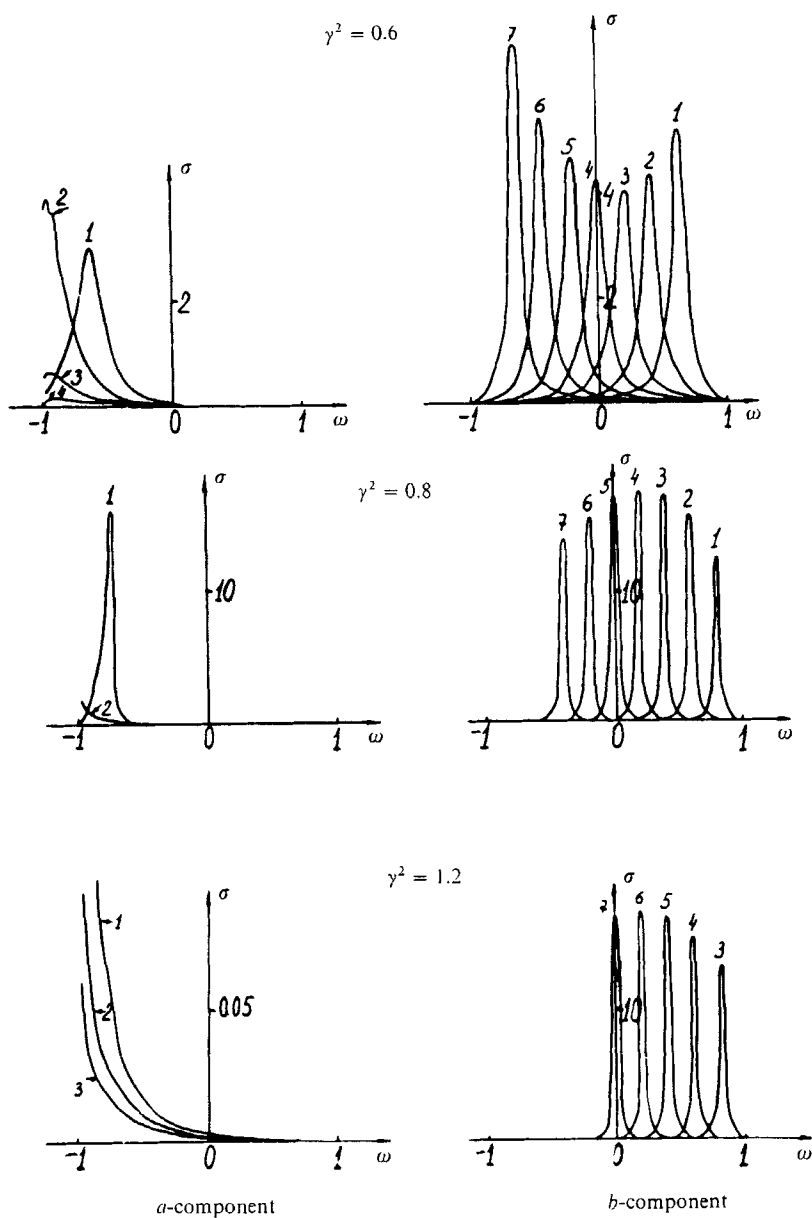


FIGURE 4 Distribution of intensity of a two-particle vibronic absorption at two polarizations. Negative frequency changes  $\Delta$  are given in units of the exciton band half-width and correspond to the marking: 1-0; 2-0.2; 3-0.4; 4-0.6; 5-0.8; 6-1.0; 7-1.2.



to pure electronic Davydov multiplets. Even this fact shows how much vibronic spectra with TS phonons are complicated compared to the case of NTS phonons where spectra are identical in both components.

The two-particle absorption intensity distribution according to Eq. (7) is described by  $\text{Im } F_\lambda(\omega)$ . Its shape for a set of values  $\Delta$  and  $\gamma^2$  is shown in Figure 4. The value  $\gamma^2 = 0$ , corresponds to the case of the NTS phonon investigated earlier.<sup>8</sup> The tendency is markedly pronounced for narrowing the two-particle absorption bands as  $\gamma^2$  approaches unity.

In the dynamical theory,<sup>1</sup> two-particle bands are  $\delta$ -functions at  $\gamma^2 = 1$ , since in this case the matrix element of the joint exciton and phonon configuration decay turns into zero and the spectrum is of quasi-one-particle character though it is located in the two-particle energy region. But even at the values  $\gamma^2$ , substantially different from unity, two-particle bands have a markedly pronounced maximum as seen from Figure 4. Exceptions are the curves corresponding to small values  $\gamma^2 \approx 0.1$  as well as to values  $\Delta$  close to the critical ones. In such cases the two-particle spectrum is either a wide band with flat maximum or a band of more complicated shape.

The zeroth moment of a spectrum does not depend on  $\Delta$  and  $\gamma$ , so the area under the calculated curves summed over one- and two-particle spectra is normalized to unity. The first moment of a spectrum defines its centre-of-gravity position  $\bar{\omega}_\lambda$  relative to the frequency  $\varepsilon_0 + \nu_0$ :  $\bar{\omega}_\lambda$  are determined by

$$\bar{\omega}_\lambda = \Delta + (-1)^\lambda 4\gamma^2 M$$

For Davydov splitting value of the  $K_1$ -transition we have, respectively,  $\Delta_1^\infty = 8\gamma^2 M = \gamma^2 \Delta_0^\infty$  where  $\Delta_0^\infty$  is Davydov splitting in the pure electronic transition.

The naphthalene- $d_0$  crystal absorption spectrum in the  $K_1$  vibronic transition region  $A_{1g} \rightarrow {}^1B_{2u} a_g$  is given in Figure 5. The narrow  $A_1$ -band ( $32229 \text{ cm}^{-1}$ ) dominates in the  $a$ -component. In the  $b$ -component, the absorption is represented by the wide band with complicated structure wholly located in the two-particle spectrum region. The analysis of the vibronic absorption showed<sup>20</sup> that the most intensive band  $\mathcal{D}_b$  ( $32260 \text{ cm}^{-1}$ ) corresponds to the phonon  $\nu_0 = 764 \text{ cm}^{-1}$  and bands I, II and III correspond to one-particle vibronic transitions with other internal phonons. The two-particle state energy spectrum is located in the region  $32240 + 32420 \text{ cm}^{-1}$ .<sup>†</sup> Hence it follows that the  $A_1$ -band is one-particle and all absorption in the  $b$ -component is of two-particle type.

When comparing the theory with experiment, we have chosen the values of two free parameters  $\Delta$  and  $\gamma^2$  so as to fit the positions of  $A_1$ -band and the  $\mathcal{D}_b$ ,

<sup>†</sup> The phonon frequency in the crystal ground state is taken to be equal to  $764 \text{ cm}^{-1}$  (Refs. 21 and 22) (in vapour  $\nu_0 = 761 \text{ cm}^{-1}$ ).

band maximum. The only  $\Delta$  and  $\gamma^2$  values meeting these requirements are  $\Delta = -0.63$  ( $-57 \text{ cm}^{-1}$ ),  $\gamma^2 = 0.20$ . As seen from Figure 3 the one-particle band exists, at these values of parameters, only in the *a*-component in accordance with the experiment. The calculated fraction of two-particle absorption in the *a*-component is about 40%. However, due to the low value of absolute intensity in the *a*-component, the wide-band two-particle absorption amplitude (cf. Figure 4 at  $\gamma^2 = 0.2$ ) is at the background level.

The calculated two-particle absorption spectrum in the *b*-component is shown in Figure 5. Due to the strong configuration mixing in the  $\mathcal{D}_b$ -band, we fail to compare the calculated and experimental bands by their absolute intensity. So, the scale along the  $\kappa$ -axis for the calculated spectrum has been chosen to make minimal the mean-square deviation of the calculated band from the experimental  $\mathcal{D}_b$ -band. As seen from Figure 5 the shape of both curves coincides fairly well.

The value  $\gamma^2 = 0.20$  found shows that the coupling between exciton and phonon under consideration is not strong. This agrees with rapid intensity decay in the luminescence band series involving this phonon,<sup>21</sup> as well as with the qualitative intensity distribution in vapour spectra.<sup>14</sup> The value of  $\Delta$  found by us turned out to be close to that of vapours  $\Delta = -59 \text{ cm}^{-1}$ ; this undoubtedly witnesses in favour of the above-performed analysis.

The similar comparison between calculated and experimental data has also been made in the  $K_1$ -transition region for the naphthalene- $d_8$ . The crystal spectrum in the  ${}^1A_{1g} \rightarrow {}^1B_{2u}a_g$  transition region is shown in Figure 6. As with the naphthalene- $d_0$  crystal, the one-particle  $A_1$ -band ( $32277 \text{ cm}^{-1}$ ) dominates in the *a*-component; the absorption in the *b*-component (except for bands I, II and III having another origin<sup>11</sup>) is fully two-particle with a markedly pronounced  $\mathcal{D}_b$ -band ( $32297 \text{ cm}^{-1}$ ). The two-particle states energy region is from  $32283 \text{ cm}^{-1}$  to  $32463 \text{ cm}^{-1}$  (in the crystal  $\nu_0 = 695 \text{ cm}^{-1}$ ).

The best fit of the experimental and calculated values of the  $A_1$  and  $\mathcal{D}_b$ -band maximum positions with respect to the two-particle spectrum low-frequency edge is achieved at the parameter values  $\Delta = -0.58$  ( $-52 \text{ cm}^{-1}$ ) and  $\gamma^2 = 0.16$  (for vapour  $\Delta = -54 \text{ cm}^{-1}$ ). Using these values one can explain the absence of the one-particle band in the *b*-component and the weakly pronounced two-particle absorption in the *a*-component at the background level (its integral intensity is about 0.46). The two-particle band obtained from the calculation is shown in Figure 6. As with the naphthalene- $d_0$  the calculated band in the spectrum under consideration fits well the experimental band and shows its main characteristics.

Thus, the general  $\mathcal{D}_b$ -band shape is well described by the theory both for the naphthalene- $d_0$  and naphthalene- $d_8$ . However, in the naphthalene- $d_0$  spectrum there is one very pronounced additional band, namely band IV (Figure 5). In the naphthalene- $d_8$  spectrum this band is likely to correspond to the

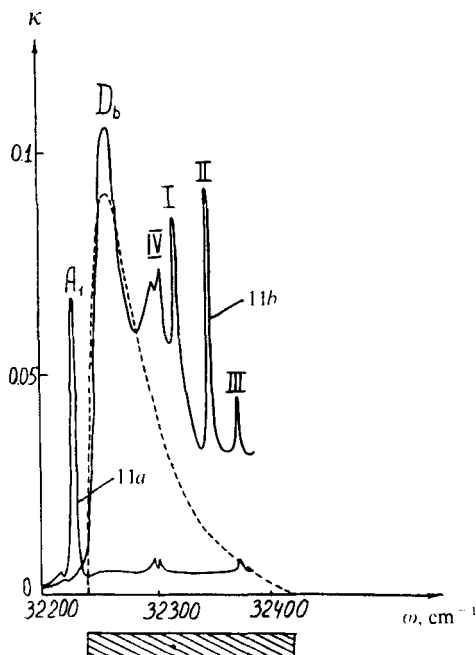


FIGURE 5 Measured (solid line) and calculated (dashed line) naphthalene- $d_0$  crystal absorption spectra in the  $K_1$ -transition region,  $T = 4.2^\circ\text{K}$ ,  $^{10,20} \Delta = -0.635$ ,  $\gamma^2 = 0.20$ . The energy region of two-particle states with the TS phonon  $\nu_0 = 764 \text{ cm}^{-1}$  is indicated under the abscissa.

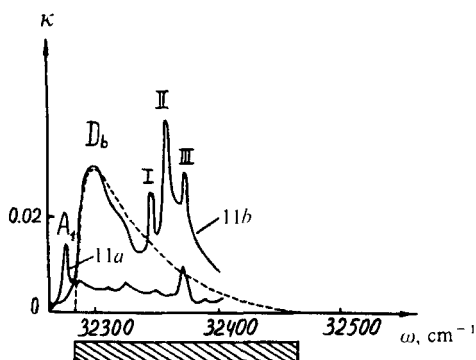


FIGURE 6 Measured (solid line) and calculated (dashed line) naphthalene- $d_0$  crystal absorption spectra in the  $K_1$ -transition region;  $T = 4.2^\circ\text{K}$ ,  $^{20} \Delta = -0.58$ ,  $\gamma^2 = 0.16$ . The energy region of two-particle states with the TS phonon  $\nu_0 = 695 \text{ cm}^{-1}$  is indicated under the abscissa.



shoulder of the  $\mathcal{D}_b$ -band. The IV-band origin is not yet clear, and temptation arises to relate it to logarithmic singularity in  $\rho(\omega)$  in the vicinity of the exciton band spectrum saddle point due to its quasi-two-dimensional structure. Such a singularity is seen in curve 2 (Figure 1), and it might be assumed that it is not revealed in the experimental curve 1.

To clear up this problem, we have calculated  $F$  for a two-dimensional problem. Using Eqs. (12) and (13) one can transform Eq. (8) to the form

$$F_\lambda(\omega) = \frac{f(0, \omega) + y_\lambda/4M}{\left\{ 1 + 2\gamma^2 - (-1)^\lambda \frac{\Delta\gamma^2}{4M} - (\Delta + 4y_\lambda)f(0, \omega) \right\}} \quad (16)$$

with  $y_\lambda = (-1)^\lambda \gamma^2 M$ . The even function  $\text{Im } f(0, \omega)$  diverges as  $\ln|\omega|$  near the saddle point: the odd function  $\text{Re } f(0, \omega)$  vanishes at  $\omega \rightarrow 0$ . It follows from Eq. (16) that near the singular point  $\omega = 0$  the function  $\text{Im } F_\lambda$  vanishes as  $\ln^{-1}|\omega|$ . An exception is a particular case  $\Delta + 4y_\lambda = 0$  when  $f(0, \omega)$  enters only the numerator of Eq. (16), so  $\text{Im } F_\lambda$  increases as  $\ln|\omega|$  at  $\omega \rightarrow 0$ .

Thus, at general values of parameters, the peak at the saddle point is absent. To clear up whether the peak arises close to it, the numerical calculation was performed by formula (16). Figure 7 displays the spectrum in the  $b$ -component at the value  $\gamma^2 = 0.2$  corresponding to the naphthalene- $d_0$ . At other values of  $\gamma^2$  the picture is similar. It is seen that the curves in Figure 7 are similar to the corresponding curves in Figure 4. The feature at  $\omega = 0$  is weak. In the cases, when extra maxima arise near  $\omega = 0$ , they are pronounced rather weakly. This, in particular, relates wholly to curve 4, corresponding to the value  $\Delta = -0.6$  which suits the naphthalene case. A sharp peak at  $\omega = 0$  on curve 2 corresponds to the above criterion  $\Delta + 4y_\lambda = 0$  (with  $\lambda = 2$  and  $4M = 1$ ): this

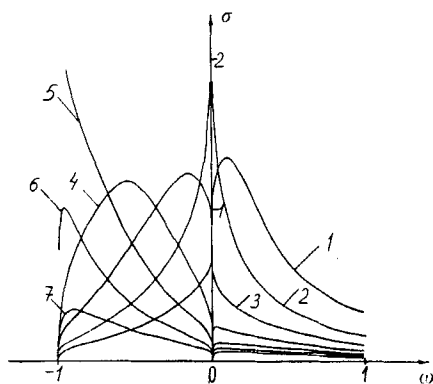


FIGURE 7 Distribution of intensity of the  $b$ -polarized two-particle vibronic absorption for the layer crystal model. Designations are the same as in Figure 4:  $\gamma^2 = 0.2$ .

curve shows no other maxima, and it has nothing in common with the experimental  $\mathcal{D}_b$ -band.

Thus, the calculation gives no reason to connect the IV-band with the saddle point, and the puzzle on the nature of this band still remains to be solved.

## 5 IMPURITY SPECTRUM

Hamiltonian (1) to (4) is easily generalized for the crystal with isotopic impurity. An independent check up of the above analysis of the intrinsic absorption in the region of  $K_1$ -transition may, therefore, be a calculation of the vibronic impurity absorption, e.g., for naphthalene- $d_0$  impurity in naphthalene- $d_8$ . The calculation was performed for the same TS phonon  $\nu_0 = 764 \text{ cm}^{-1}$  for the restricted crystal region in the plane lattice approximation. In the lowest approximation four nearest neighbours (first coordinational sphere) and in the next one twelve neighbours (three coordinational spheres) were taken into account. The calculation, was based on the hamiltonian (1)–(4) supplemented by two terms. The first of them  $\Delta_{\text{ex}} a_0^+ a_0$  with  $\Delta_{\text{ex}} = -115 \text{ cm}^{-1}$  describes the isotopic shift for exciton and the second  $\Delta_{\text{ph}} b_0^+ b_0$  with  $\Delta_{\text{ph}} = 69 \text{ cm}^{-1}$  for phonon on the impurity site  $\mathbf{r} = 0$ . Some corrections were made taking into account the difference in parameter values  $\Delta$  and  $\gamma^2$  in naphthalenes  $d_0$  and  $d_8$  ( $\Delta = -57$  and  $-52 \text{ cm}^{-1}$ , and  $\gamma^2 = 0.20$  and  $0.16$ , resp.).

The results for some lowest levels of the system are summarized in Table I; total intensity of the vibronic transition in the intrinsic spectrum calculated per one molecule is taken as the intensity unit. The results are more easily understood when singling out two configurations which contribute predominantly into these states. The configuration with both exciton and phonon being on the impurity molecule corresponds to the energy  $-115 + 69 - 57 = -103 \text{ cm}^{-1}$ . The configuration with exciton being on the impurity molecule and phonon on one of the host molecules corresponds to the energy  $-115 \text{ cm}^{-1}$ . The remainder configurations have a substantially higher energy. Hence, the lowest level of the first approximation as well as three lowest levels of the second approximation are the first terms ( $m = 1, 2, \dots$ ) of the series corresponding to the states when exciton is bound predominantly at the impurity centre and TS phonon is moving at an ever-increasing distance from it. From Table I it follows that the binding energy for this series is very low: it is about  $\delta\varepsilon = -1.5$  to  $-2 \text{ cm}^{-1}$ . The intensities of successive bands decrease rapidly since the total oscillator strength of vibronic transition arises from the joint configuration of exciton and phonon. The limit of this succession corresponds to the frequency  $\omega_\infty = \omega_{K'_0} + \nu_0$  where  $\omega_{K'_0}$  is the frequency of the impurity electronic  $K'_0$  band, and  $\nu_0$  is  $695 \text{ cm}^{-1}$  ( $d_8$  is host). If the

TABLE I  
Calculated positions and intensity values of impurity absorption bands of naphthalene- $d_0$  in  $d_8$  in the  $K_1$ -transition region

Band designation and quantum number	Dominating configuration energy <sup>a</sup> ( $\text{cm}^{-1}$ )	First approximation		Second approximation	
		Energy <sup>a</sup> ( $\text{cm}^{-1}$ )	Intensity <sup>b</sup> $\ a\ b$	Energy <sup>a</sup> ( $\text{cm}^{-1}$ )	Intensity <sup>b</sup> $\ a\ b$
$K'_1$	-103	-110.7	1.28	-111.4	1.381
$m = 0$					
$K''_1, K'''_1 \dots$	-115	-131.6	0.33	-134.2	0.53
$m = 1, 2, \dots \infty$					
				-132.88	0.015
				-132.83	0.005
					0.017

<sup>a</sup> Energy is counted off the term of separated vibronic configuration of the host  $\epsilon_0 + \nu_0$  which equals to  $\omega = 32167 \text{ cm}^{-1}$ .

<sup>b</sup> Intensity is calculated per one molecule and is expressed in terms of fractions of total intensity of the host  $K_1$ -transition in the corresponding spectrum component.

experimental value  $\omega_{K'_0}$  (Ref. 23) is used, then  $\omega_\infty = 32037 \text{ cm}^{-1}$  which constitutes  $-130 \text{ cm}^{-1}$  counted off the term of separated vibronic configuration of the host crystal. This value, within the accuracy of determining the energy  $\omega_{K'_0}$ , is in agreement with the calculation for  $m = \infty$ .

The next band ( $-111.4 \text{ cm}^{-1}$  in the second approximation) is, in fact, the zeroth term of this series ( $m = 0$ ) falling out entirely in frequency of series regularity. In the quantum state, corresponding to this band, the completely joint configuration dominates so that exciton and phonon are on the impurity molecule. As a result band is to be observed in the spectrum with the highest intensity. The deviation of its intensity from unity (in both spectrum components; see Table I) is due to the fact that exciton-phonon wave function is partly extended outside the impurity cite.

From Table I it is seen that the convergence of results for energies is rather good. As to the accuracy of results for intensities (especially for the  $K''_1$ -band), it is far less.

By analogy with the accepted<sup>6, 24, 25</sup> designation of impurity bands in the region of vibronic transitions with NTS-phonon ( $M'$ ,  $M''$ , etc.) we denote the band with  $m = 0$  as  $K'_1$ , and bands with  $m \geq 1$ —as  $K''_1$ ,  $K'''_1$  and so on. The difference is that in the primed  $M$ -states, a phonon is in fixed position on one of the sites, while in the primed  $K_1$ -sites, it moves over the crystal (mainly near the definite coordinational sphere).

On the higher energy side there is the host  $A_1$ -band. Our calculation accuracy is insufficient to ascertain whether it is preceded by the local state in which the vibron as the whole is weakly bound at the impurity centre.

Figure 8 displays the experimental data on the impurity absorption of naphthalene— $d_0$  in  $d_8$  in the  $K_1$ -transition region. In this figure also are shown theoretical positions of impurity bands obtained as a sum of energies given in Table 1 and the experimental value of the vibronic term  $\epsilon_0 + \nu_0$  of the host crystal. The arrow  $A_1$  indicates the calculated position of the  $A_1$ -band according to Section 4.

Comparison of spectra 1 and 2 in Figure 8 shows that even at the concentration of  $d_0$  equal to 2%, the band  $K'_1$  is apparently pronounced. With further increasing in concentration to 10% the intensity of this band increases nearly linearly, and its maximum is shifted somewhat to lower frequencies. Such a behaviour is very much reminiscent of that for the impurity  $M'$ -bands with  $\Delta_{\text{ex}} < 0$ .<sup>25</sup> The assignment of this absorption as the  $K'$ -band (i.e. with the state  $m = 0$ ) is beyond any doubt.

The subtraction of the  $K''_1$  band on curve 2 can be done only questionably since the change in absorption is within the experimental error shown in Figure 8 by bars. The error is found by the change in the  $\kappa$  scale for different crystals. But on curve 3 (concentration is 5%) the maximum in the  $K''_1$ -band region is pronounced apparently. It is of interest that this maximum does not

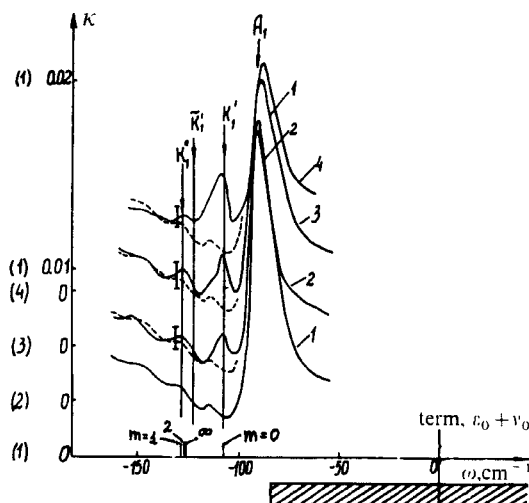


FIGURE 8 The  $a$ -component of the naphthalene- $d_8$  crystal absorption spectra with impurity  $d_0$  in the  $K_1$ -transition region (experimental data are obtained by A. V. Leiderman). The curves correspond to the following concentration values of  $d_0$ : 1—0%; 2—2%; 3—5%; 4—10%. The curves are shifted respectively to one another along the vertical and the points (1) 0, (2) 0, (3) 0 and (4) 0 correspond to a zero reading of intensities of the curves 1, 2, 3 and 4, respectively. The absolute scale is the same for all the curves and is indicated for curve 1. Energy is reckoned from the crystal-solvent vibronic term  $\epsilon_0 + \nu_0$  ( $32167 \text{ cm}^{-1}$ ). Beneath the abscissa is shown the region of two-particle states with the TS phonon  $\nu_0 = 695 \text{ cm}^{-1}$  for  $d_8$  crystal. The arrows denoted  $A_1$ ,  $K'_1$  and  $K''_1$  indicate the calculated positions of corresponding bands,  $K'_1$  corresponds to the position of the impurity  $K'_1$  band, calculated by Eq. (15). The quantum number  $m$  for the impurity states are indicated above the abscissa. The dashed line repeats the host absorption.

increase on further and becomes smoothed (curve 4), which seems to be quite natural since the structure corresponding to separated configurations must be the least steady one. The ratio of the  $K''_1$ - and  $K'_1$ -band intensities, by Table I, is  $\sim 30\%$ ; this value does not contradict the experimental data in Figure 8 at low concentration ( $\approx 5\%$ ).

It should be emphasized in conclusion that an excellent agreement of theoretical and experimental positions of the  $K'_1$  and  $K''_1$  bands is all the more convincing that we had no free parameters when calculating them.

## 6 COMPOUND VIBRONS

Quite similarly to the impurity vibronic  $K_1$ -spectra, one can calculate the spectrum of compound  $MK_1$  vibron including one NTS and one TS phonons (with frequency changes  $\Delta = -89 \text{ cm}^{-1}$  and  $\Delta = -57 \text{ cm}^{-1}$ , respectively) in a neat crystal. The site on which NTS phonon is localized acts here as the impurity site and the difference is mainly that the placing of two phonons on

the same site does not result in the change of phonon energy (i.e.  $\Delta_{ph} = 0$  within the harmonic approximation). Therefore, classification of states is like that for the impurity vibron hence we label the bands in an analogous way.

The results of calculation are shown in Table II. Here the band corresponding to the  $m = 0$  term of the series has the lowest frequency. For it the completely joint configuration predominates, as before (both phonons and exciton are on the same site), so this band is the strongest. As to the other states, where separated configurations of phonons are predominant, they must have extremely low intensities and thus are hardly to be detected experimentally.

According to the calculation, the  $(MK_1)'$  band is to be located at frequencies  $32680\text{ cm}^{-1}$  and  $32717\text{ cm}^{-1}$  in the  $d_0$  and  $d_8$  crystals, respectively. Two apparently pronounced bands at  $32674\text{ cm}^{-1}$  and  $32678\text{ cm}^{-1}$  are observed in the  $d_0$  crystal<sup>26</sup> experimentally, their assignment has not yet been established. One of them should be assigned to the  $(MK_1)'$ -transition. The spectroscopic analysis which will be described elsewhere<sup>26</sup> shows that the first band should probably be identified with the  $(MK_1)'$  band. In the  $d_8$  crystal the band at  $32718\text{ cm}^{-1}$  is observed.<sup>26</sup> Its position coincides extremely well with the theoretically calculated one. Since there are no other bands nearby this identification seems to be unambiguous.

It is also of some interest to discuss the compound vibron  $2\nu_0$  (overtone). For the phonon  $\nu_0 = 764\text{ cm}^{-1}$  in the  $d_0$  crystal a rather large frequency change  $2\Delta = -114\text{ cm}^{-1}$  corresponds to the joint overtone configuration so the one-particle state will possess large binding energy. In this case the level shift caused by repulsion from the bottom of three-particle state spectrum is to be about the same as for impurity exciton with equivalent  $\Delta_{ex}$  (this shift value is expected to be about  $10\text{ cm}^{-1}$ ). A more precise calculation has not been performed so far. The great  $2\Delta$  value results in the fact that  $A_2$  and  $B_2$  one-particle bands will exist (and dominate) in the two-phonon  $K_2$ -transition in both spectrum components (in contrast to the  $K_1$ -transition). Matrix elements, corresponding to the resonance simultaneous transfer of exciton and two TS phonons from site to site are  $M_{2n\alpha m\beta} = (\gamma^4/2) M_{0n\alpha m\beta}$ , so Davydov splitting in doublets  $A_2 B_2$  and  $A_0 B_0$  are simply interrelated:  $\Delta_2^{\beta} \approx (\gamma^4/2) \Delta_0^{\beta} \approx 3\text{ cm}^{-1}$  ( $1.6\text{ cm}^{-1}$  for the  $d_8$  crystal). Such a splitting of  $A_2$  and  $B_2$ -bands in the spectrum region discussed may hardly be observed. By analogy to the compound vibron such a band can be designated as  $(KK)'$ .

In the  $d_0$  crystal two non-split bands  $32949$  and  $32956\text{ cm}^{-1}$  are located in the region of the expected position of the  $A_2$ - $B_2$  doublet. The analysis of intensities of these bands shows that the second band, relatively weaker, of them should be most likely assigned as the band  $(KK)'$ . In the  $d_8$  crystal the non-split band  $32954\text{ cm}^{-1}$  can be identified in such a manner (see, however, remarks below on this band position).

TABLE II  
Calculated position and intensity values of lower absorption bands for the compound  $MK_1$ -vibron in the neat naphthalene  $-d_0$

Band designation quantum number	Dominating configuration energy <sup>a</sup> (cm <sup>-1</sup> )	First approximation		Second approximation	
		Energy <sup>a</sup> (cm <sup>-1</sup> )	Intensity <sup>b</sup>	Energy <sup>a</sup> (cm <sup>-1</sup> )	Intensity <sup>b</sup>
$(MK_1)^r$ $m = 0$	-146	-152.5	0.93	-153.5	0.91
$(MK_1)^r, (MK_1)^m, \dots$ $m = 1, 2, \dots, \infty$	-89	-106.5	0.007	-111.6 -109.7 -109.5	0.009 0.0007 0.0004

<sup>a</sup> Energy is counted off the vibronic term  $v_0 + v_0^1 + v_0^2$  and  $v_0$  are the NTS and TS phonon frequencies in the ground state.

<sup>b</sup> Intensity is expressed in terms of fractions of total intensity of the  $MK_1$ -transition in any spectrum component.

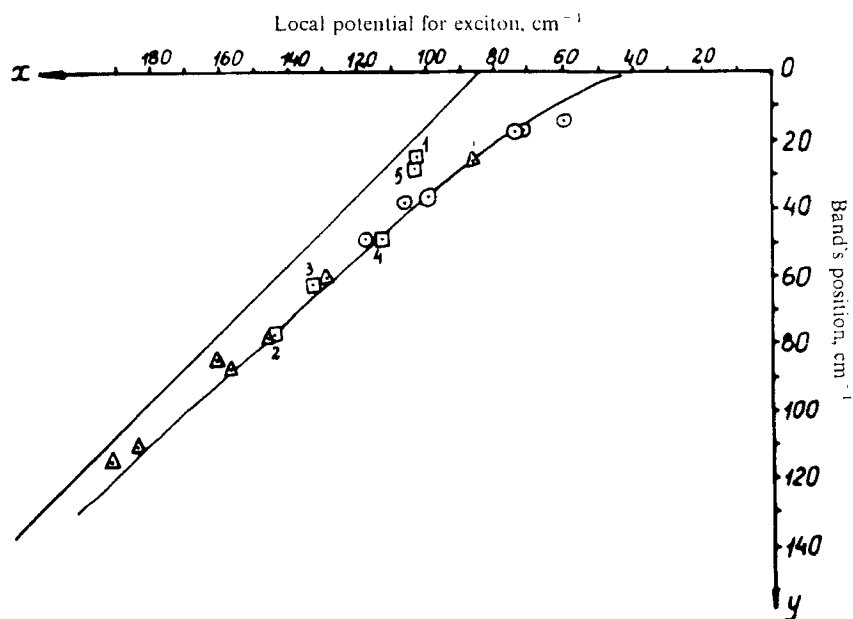


FIGURE 9 Band position of local and one-particle (electronic and vibronic) absorption in neat and isotope-impurity naphthalene crystals depending on the potential energy of exciton in the corresponding states.  $\odot$  are the  $K'_0$  bands of purely electronic impurity absorption;<sup>2,3</sup> the position is measured from the exciton band bottom.  $\triangle$  are the  $M'$  bands of vibronic absorption with one NTS phonon and the naphthalene crystal  $M$ -band;<sup>2,3</sup> the position is measured from the bottom of two-particle state spectrum.  $\square$  are the bands of compound tones and overtones. 1 is the  $K'_1$ -band of vibronic absorption with the TS phonon for the impurity  $d_0$  in the  $d_8$  crystal; the position is measured from the bottom of two-particle spectrum. 2 and 3 are the  $(MK_1)'$ -bands of one-particle absorption in the compound vibronic transition of the  $d_0$  and  $d_8$  crystals, respectively; 4 and 5 are the  $(KK)'$  bands of one-particle overtone vibronic absorption of the  $d_0$  and  $d_8$  crystals, respectively; band positions are measured from the bottom of three-particle state spectrum.

## 7 POSITION OF VIBRONIC BANDS

To value concordance of the above data, we display in Figure 9 the summary data on the position of the number of bands in spectra of naphthalenes. One group of points corresponds to the position of  $K'_0$  isotopic impurity bands in the pure electronic spectrum. In this case, on the abscissa the local potential of the defect, i.e. the isotopic shift  $\Delta_{ex}$  determining the level position by the equation analogous to (15), is plotted. The second group of points corresponds to  $M$  and  $M'$  vibronic bands. The local exciton potential, in this case equal to the frequency change  $\Delta$  for the intrinsic  $M$ -band or to the sum  $\Delta + \Delta_{ex}$  for impurity  $M'$ -bands, is also plotted on the abscissa. The third group of five points corresponds to the above  $K'_1$  and  $(MK_1)'$  and  $(KK)'$ -bands. For them,



the energy of completely joint configuration was plotted on the abscissa (cf. Tables I and II).

Within the framework of the dynamical theory, the two first groups of points are defined by the same Eq. (15), so they must lie on the same curve. From Figure 9 it is seen that this actually occurs.<sup>23</sup>

The case is somewhat different with the third group of bands which due to the term  $H_{\text{int}}^{(2)}$  in hamiltonian (1) are defined by more complicated equations. One can see however the positions of the bands 2, 3 and 4 corresponding to the large values  $|\Delta + \Delta^1|$  and  $2|\Delta|$  deviate insignificantly from the curve. In particular, the positions of the  $(MK'_1)$ -bands 2 and 3, calculated in Section 6, differ from that obtained by formula (15) by  $1.2 \text{ cm}^{-1}$  and  $2.3 \text{ cm}^{-1}$  respectively.

The observed shift in the position of the point 1 is quite natural, since the  $K'_1$  band is repelled up from the group of levels with  $m \geq 1$  located below it (cf. Table I). At the same time, this band's position, as shown in Section 5, coincides with that calculated by the rigorous theory. So, the strong shift of band as compared to the results obtained by Eq. (15) is an excellent exhibition of the TS phonons mobility effect and of the influence of the term  $H_{\text{int}}^{(2)}$ .

The observed strong shift of the  $(KK')$ -band in the  $d_8$  crystal (point 5) is however obscure. We have no ideas concerning a model which could explain qualitatively such a substantial level shift. A rigorous calculation of the level position as well as the discussion of some extra mechanisms (e.g. intramolecular anharmonism) are called for. Therefore, the assignment of the band  $32954 \text{ cm}^{-1}$  as the  $(KK')$  band must be considered tentative.

## 8 CONCLUSION

As far as we know, this paper is the first, where the complete calculation and quantitative analysis of vibronic spectrum with TS phonon was carried out. Preliminary results of our analysis were reported in Ref. 27. The previous calculations in Refs. 1, 2 and 3 were concerned with one-dimensional models only.

The calculation reveals clearly the qualitative regularities of the spectrum. Thus, wide two-particle bands arising at the small exciton-phonon coupling constants  $\gamma^2 \ll 1$  (like that for NTS phonons), are quickly narrowed with increasing  $\gamma^2$ . Even at  $\gamma^2 \approx 0.4$ , two-particle bands possess a simple regular shape with the half-width substantially less than the exciton band width. The exceptions to this rule occur only for some frequency change  $\Delta$  ranges mainly in the vicinity of  $\Delta_{\text{cr}}$  corresponding to the one-particle band appearance. At  $\gamma^2 = 1$ , in accordance with the general theory, two-particle bands become  $\delta$ -shaped. It is very important that over a wide range of parameters the one-

particle absorption exists only in one spectrum component; the absorption in the other is totally two-particle.

The application of the theory to the  $K_1$ -transition in the naphthalene crystal proved to be quite successful. At the value of  $\Delta$  close to that obtained from the vapour spectrum and at the value of  $\gamma^2 = 0.2$ , being in agreement with other data, it has been possible to obtain a rather good description of the spectrum in both components, and namely the correct position of one-particle  $A_1$ -bands and both the correct position and the shape of two-particle  $\mathcal{D}_b$ -band. The spectrum of isotope impurity absorption in the  $K_1$ -transition region have also been calculated. The calculation has revealed the existence of a series of bands corresponding to the impurity-vibronic complex. The first two bands of the series were found experimentally.

The application of the theory to compound vibronic transition including TS and NTS phonons proved to be successful, as well. A number of the observed bands were identified, although the assignment for some of them is not unambiguous and further work is to be done.

When performing the calculations followed by the analysis of experimental data, the tendency is clearly revealed for all-increasing predominance of the one-particle absorption in the region of compound (two- and more-phonon) transitions. This is due to the all-increasing value of binding energy of completely joint configurations. From this it follows that in the regions of many-phonon vibronic transitions, the crystal absorption spectrum becomes more like the molecular one even though in the region of one-phonon vibronic transitions these both spectra are substantially different.

We consider the success in interpretation of intrinsic and impurity vibronic spectra as quantitative corroboration of the dynamical theory of vibronic spectra forming the basis of our calculations.

### Acknowledgements

The authors take pleasure in acknowledging very helpful discussions with Prof. V. L. Broude. We should also like to thank Mr. A. V. Leiderman and Dr. I. P. Terenetskaya for providing us with the data of their experimental investigations of absorption spectra, and Mr. A. M. Tsyganok for his help in preparing the English version of the manuscript.

### References

1. E. I. Rashba, *ZhETF*, **50**, 1164, 1966; *ZhETF*, **54**, 542, 1968 (*Sov. Phys.-JETP*, **23**, 708, 1966; *Sov. Phys.-JETP*, **27**, 292, 1968).
2. M. R. Philpott, *Journ. Chem. Phys.*, **51**, 2616, 1969.
3. A. S. Davydov and A. A. Serikov, *Phys. Stat. Sol.*, **44**, 127, 1971.
4. L. Valkunas and V. I. Sugakov, *Ukr. Fiz. Zh.*, **17**, 1575, 1972.
5. H. Sumi, *Journ. Phys. Soc. Jap.*, **38**, 825, 1975.
6. V. L. Broude, E. I. Rashba, and E. F. Sheka, *Phys. Stat. Sol.*, **19**, 395, 1967.

7. E. F. Sheka, *Usp. Fiz. Nauk*, **104**, 593, 1971 (*Sov. Phys. Uspekhi*, **14**, 484, 1972).
8. N. V. Rabinkina, E. I. Rashba, and E. F. Sheka, *FTT*, **12**, 3569, 1970 (*Sov. Phys.-Solid State*, **12**, 2898, 1971).
9. N. I. Ostapenko and M. T. Shpak, *ZhETP, Pisma*, **16**, 513, 1972.
10. A. F. Prikhotko and M. S. Soskin, *Opt. i Spekt.*, **13**, 522, 1962; M. S. Soskin, *Ukr. Fiz. Zh.*, **6**, 806, 1961.
11. E. F. Sheka and I. P. Terenetskaya, *Chem. Phys.*, **8**, 99, 1975.
12. S. D. Colson, D. M. Hanson, R. Kopelman, and G. W. Robinson, *Journ. Chem. Phys.*, **48**, 2215, 1968.
13. H.-K. Hong and R. Kopelman, *Journ. Chem. Phys.*, **55**, 724, 1971.
14. D. P. Craig, J. M. Hollas, M. F. Redies, and S. C. Wait, *Phil. Trans. Roy. Soc. L*, **253A**, 543, 1961.
15. D. P. Craig and P. C. Hobbins, *Journ. Chem. Soc. L*, **539**, 2302, 1955.
16. J. G. Angus and G. S. Morris, *Mol. Cryst. Liq. Cryst.*, **11**, 257, 1970.
17. H. Sponer and C. Cooper, *Journ. Chem. Phys.*, **23**, 646, 1955.
18. A. F. Prikhotko, *ZhETP*, **19**, 383, 1949.
19. V. I. Sugakov, *Opt. i Spekt.*, **28**, 695, 1970.
20. I. P. Terenetskaya, *Opt. i Spekt.*, **36**, 518, 1974.
21. V. L. Broude, E. F. Sheka, and M. T. Shpak, *Opt. i Spekt.*, *Sbornik Luminesc.*, p. 102, 1963.
22. M. Suzuki, T. Yokoyama, and M. Ito, *Spectrochim. Acta*, **24A**, 1991, 1968.
23. E. F. Sheka, *FTT*, **12**, 1167, 1970 (*Sov. Phys.-Solid State*, **12**, 911, 1970).
24. V. K. Dolganov and E. F. Sheka, *FTT*, **11**, 2427, 1969 (*Sov. Phys.-Solid State*, **11**, 1962, 1970).
25. E. F. Sheka and I. P. Terenetskaya, *FTT*, **12**, 720, 1970 (*Sov. Phys.-Solid State*, **12**, 558, 1970).
26. T. A. Krivenko, A. V. Leiderman, I. P. Terenetskaya, and E. F. Sheka, *Opt. i Spekt.*, **45**, 435, 1978.
27. T. A. Krivenko, E. I. Rashba, and E. F. Sheka in *Sovremyonnye problemy spektroskopii molekulyarnykh kristallov* (*Modern problems on molecular crystal spectroscopy*) Naukova Dumka, Kiev, p. 23, 1976.